Oxidative stress characterizes the dysfunction of thermogenic adipose tissue in a mouse model of down syndrome

Oxidative stress characterizes the dysfunction of thermogenic adipose tissue in a mouse model of Down Syndrome

Castelli S[a,b], Tramutola A[c], Perluigi M[c], Bacalini MG[d], Ciriolo MR[b,e], Ciccarone F[b,e,*]

a. Department for the Promotion of Human Science and Quality of Life, San Raffaele Open University, Via di Val Cannuta, 247, 00166 Rome, Italy
b. IRCCS San Raffaele Roma, 00166 Rome, Italy
c. Department of Biochemical Sciences "A. Rossi-Fanelli", Sapienza University of Rome, 00185 Rome, Italy
d. Department of Biomedical and Neuromotor Sciences (DIBINEM), University of Bologna, Bologna, Italy
e. Department of Biology, University of Rome Tor Vergata, 00133 Rome, Italy

*Corresponding author: Ciccarone F. fabio.ciccarone@uniroma2.it

Abstract

Down syndrome (DS) is associated with intellectual disability and multiple metabolic abnormalities, including obesity and early-onset type 2 diabetes. Gene dosage effects resulting from trisomy 21 may contribute to metabolic dysregulation in DS by impairing the function of key organs involved in systemic energy homeostasis. Brown and beige adipocytes, which are specialized for thermogenesis, dissipate energy through the oxidation of fatty acids and glucose, and are thus protective against metabolic diseases.

In this study, we investigated the thermogenic potential of brown adipose tissue (BAT) in the Ts2Cje mouse model of DS. DS BAT exhibited morphological and functional signs of impairment, including enlarged lipid droplets and reduced expression of thermogenic proteins, consistent with a whitening phenotype. These changes were accompanied by decreased mitochondrial fission, suppressed triglyceride and glucose catabolism, and blunted insulin signaling. Subcutaneous adipose tissue, in which beige adipocytes are distributed, also showed signs of degeneration in DS mice, with a marked increase in senescence and inflammatory markers. In both adipose depots, superoxide dismutase 1 (SOD1), a gene triplicated in DS, was significantly upregulated and positively correlated with markers of lipid peroxidation and adipose tissue dysfunction.

Together, these findings suggest that oxidative stress, driven in part by SOD1 overexpression, may compromise the thermogenic function of adipose tissue in DS, thereby contributing to the development of metabolic disorders in this condition.

Keywords

Brown adipose tissue, BAT whitening, SOD1, Trisomy 21, lipid peroxidation

Abbreviations

4-HNE, 4-Hydroxynonenal; AKT, Protein kinase B; ASPA, aspartoacylase; ATGL, Adipose triglyceride lipase; ATP5A, ATP synthase subunit A; BACH1, BTB and CNC homologous protein 1; BAT, brown adipose tissue; CAT, Catalase; CHOP, C/EBP homologous protein; DRP1, Dynamin related protein 1; DS, Down syndrome; Eu, Euploid; FSP1, ferroptosis suppressor protein 1; GPX4, glutathione peroxidase 4; HIF1α, Hypoxia-inducible factor 1-alpha; HSL, hormone sensitive lipase; IR, insulin receptor; LDs, lipid droplets; MNF2, Mitofusin 2; NAA, N-acetylaspartate; NAT8L, N-acetyltransferase 8 like; NDUF8B, NADH:Ubiquinone Oxidoreductase Core Subunit S8; OPA1,

optic atrophy 1; PDH, Pyruvate dehydrogenase; SDHB, Succinate dehydrogenase B; SOD1, Superoxide dismutase 1; SOD2, Superoxide dismutase 2; sWAT, subcutaneous white adipose tissue; ROS, reactive oxygen species; TFAM, mitochondrial transcription factor A; UCP1, Uncoupling protein 1.

Introduction

Down syndrome (DS), the most common chromosomal aneuploidy in humans, results from the presence of an extra full or partial copy of chromosome 21. A prevailing hypothesis in DS pathophysiology is genomic imbalance, primarily driven by the overexpression of genes located on the trisomic chromosome. Despite tissue-specific variability in gene expression, gene dosage effects are believed to underlie many DS phenotypes, including its clinical and metabolic heterogeneity [1]. Oxidative stress is a hallmark of DS and has been attributed in part to the triplication of genes such as superoxide dismutase 1 (*SOD1*), which codifies for the cytosolic superoxide dismutase, and BTB Domain And CNC Homolog 1 (*BACH1*), a transcriptional repressor involved in redox regulation and ferroptosis [2]. These genes contribute to a redox imbalance that is evident across multiple tissues and may play a central role in DS-associated dysfunctions. In addition to cognitive and morphological impairments, individuals with DS exhibit significant metabolic alterations, prompting the characterization of DS as a "metabolic disease" [3]. Epidemiological studies have reported a higher prevalence of obesity, insulin resistance, and early-onset type 2 diabetes (T2D) in the DS population compared to the general population [4]. Similar features, including hyperglycemia/hyperinsulinemia, and tissue-specific inflammation/fibrosis, are recapitulated in the Ts65Dn mouse model of DS [5].

While WAT accumulates fatty acids and releases them upon energy request from other organs, brown adipose tissue (BAT) contributes to whole-body energy homeostasis and insulin sensitivity by dissipating energy through non-shivering thermogenesis. This process can also occur within subcutaneous WAT (sWAT) due to the presence of a specific class of cells called beige adipocytes (WAT browning). When stimulated by cold or β3-adrenergic signals, both brown and beige adipocytes upregulate the expression of uncoupling protein 1 (UCP1) to dissipate mitochondrial protein gradient. These features of thermogenic adipocytes confer protection against several metabolic disorders, including obesity, T2D, and dyslipidaemia [6]. Conversely, obesity leads to a substantially reduced activity in BAT, mainly due to the conversion of brown adipocytes to white-like cells (BAT whitening) [6]. This phenomenon is strongly associated with oxidative stress, hypoxia

and inflammation [7,8]. In the last years, the alteration of BAT has been evidenced in several neurological disorders characterised by systemic dysmetabolism [9,10].

In this study, we explored BAT function in the Ts2Cje (Ts2) mouse model of DS. Our findings reveal, for the first time, a significant impairment of thermogenic adipose tissue in this model, closely associated with oxidative stress and an imbalance in antioxidant defense mechanisms.

Materials and Methods

Animals

Ts2Cje (Rb (12.Ts171665Dn)2Cje) mice are a well-established mouse model of DS characterized by a triple copy of a Robertsonian fusion chromosome carrying the distal end of Chr16 and Chr12. Parental generations were purchased from Jackson Laboratories (Bar Harbour, ME, USA). The mouse colony was obtained by a crossbreed of Ts2Cje trisomic females with euploid (B6EiC3SnF1/J) F1 hybrid males (Eu), producing litters containing both trisomic (Ts2Cje) and euploid (Eu) offspring. The parental generations of Eu mice were purchased from Jackson Laboratories (Bar Harbour, ME, USA). Pups were genotyped to determine trisomy by standard PCR. Mice were accommodated in clear Plexiglas cages (20 × 22 × 20 cm) under standard laboratory conditions with a temperature of 22 ± 2 °C and 70% humidity, a 12-h light/dark cycle, and free access to food and water. In this study we used six 5-month-old euploid male mice and six 5-month-old Ts2Cje male mice.

Histochemical analysis

To evaluate adipocyte morphology, explanted BAT tissues were embedded in paraffin. Successively, paraffin-embedded tissues were cut into 7 mm sections and stained with haematoxylin and eosin (H&E) before the microscopic analysis. For each section, the lipid droplet area was measured in at least three fields with ImageJ. An average score of each sample was used for the correlation.

SA-β gal staining

The sAT SA-β gal staining was carried out after sWAT samples were fixed in 4% paraformaldehyde and incubated for 4 h at 37°C in a pH 6.0 β-gal staining solution (1 mg/ml 1,5-bromo-4-chloro-3-indolyl β-D-galactopyranoside, 5 mM potassium ferrocyanide, 5 mM potassium ferricyanide, 150 mM NaCl, 2 mM $MgCl_2$). Images acquired by a digital camera.

Western blot analysis

BAT and WAT samples were homogenized by IKA T25, DIGITAL ULTRA-TURRAX in 1 ml of lysis buffer (50 mM Tris-HCl, pH 7.4, 150 mM NaCl, 1 mM EDTA, 1% Triton X-100, 0.5% sodium deoxycholate, 0.1% SDS, 10 mM NaF, 5 mM Sodium Pyrophosphate, 2 mM Sodium Orthovanadate) supplemented with protease inhibitor cocktail (AMRESCO). The homogenate was centrifuged at 10000×g for 15 min at 4°C and then sonicated (BRANSON ULTRASONICS CORPORATION). Lowry method was used to evaluate protein concentration and after electrophoresis by SDS-PAGE was performed. The following primary antibodies were used: 4-NHE (R&D Systems); AKT, p-AKT, BACH1, FSP1, GPX4, HIF1α, PDHE1α, TFAM (Santa Cruz Biotechnology); ASPA (Novus Biologicals), ATGL, CHOP, HSL, p-p65 (S536), p65, p21, SOD2, UCP1 (Cell Signaling Technology), ATP5A, CAT, NDUFB8, SOD1, SDHB (Abcam); DRP1, OPA1 (BD transduction laboratories); NAT8L (Sigma-Aldrich), MFN2 (Abnova), p-PDHE1α (S300) (Calbiochem). Following the incubation with specific secondary antibodies (Bio-Rad), the signal was detected using Fluorchem Imaging System (Alpha Innotech) after incubation with Clarity Max ECL Western Blotting Substrates (BioRad). Densitometry analyses were performed by ImageJ and the obtained values were used to calculate the Pearson correlation coefficient (r).

Data analysis

Data are presented as mean ± SD. Unpaired Student's *t*-test (two-group comparison) was used to analyse data that are shown as fold change relative to sample 1 of Eu (Eu1). Experiments were performed on six mice per group. Statistical analysis was performed by GraphPad Prism 8 software. Comparisons were considered statistically significant at $P \leq 0.05$.

RESULTS

Brown adipose tissue in Ts2Cje mice exhibits whitening features and altered mitochondrial dynamics

Thermogenic adipose tissue analysis was conducted in 5-month-old Ts2 mice, which exhibited a significant reduction in brown adipose tissue (BAT) weight (Figure 1A) and an increase in visceral fat mass compared to age-matched euploid (Eu) controls (Figure 1B). Histological examination of BAT from Ts2 mice revealed a marked enlargement of lipid droplets, consistent with hypertrophy of brown adipocytes (Figure 1C, D). These morphological changes, together with the significant downregulation of UCP1 –a key marker of BAT thermogenic function– indicate the onset of BAT whitening in the DS model (Figure 1E, F). Importantly, the reduction in UCP1 expression was not attributable to a global loss of mitochondrial content. Levels of mitochondrial transcription factor A (TFAM) (Figure 1E, G), as well as representative subunits of the electron transport chain (ETC) complexes I (NDUFB8) and II (SDHB), remained unchanged (Figure 1H, J, K). Intriguingly, the ATP synthase subunit ATP5A (complex V) was upregulated in Ts2 mice (Figure 1H, I), suggesting an adaptive response of the oxidative phosphorylation machinery.

To investigate whether these mitochondrial alterations reflected changes in mitochondrial dynamics, we assessed the expression of key proteins involved in fusion and fission processes. BAT from Ts2 mice showed increased levels of Mitofusin 2 (MFN2), a mediator of outer mitochondrial membrane fusion (Figure 1L, M), and decreased expression of the fission protein Dynamin-related protein 1 (DRP1) (Figure 1N, O). The corresponding increase in the mitochondrial fusion index further supports a shift towards a fused mitochondrial network in DS BAT (Figure 1P). These findings were corroborated by analysis of the inner mitochondrial membrane fusion protein optic atrophy 1 (OPA1). In particular, the balance between long (L-OPA1) and short (S-OPA1) isoforms, which regulates cristae remodeling and mitochondrial function, was skewed in favor of L-OPA1 in Ts2 mice (Figure 1Q, R), indicating a preference toward fusion.

Together, these data suggest that BAT in DS is not only structurally and functionally compromised but also undergoes significant remodeling of mitochondrial dynamics. These alterations may impair mitochondrial efficiency and contribute to increased oxidative stress, with potential repercussions for systemic metabolic homeostasis.

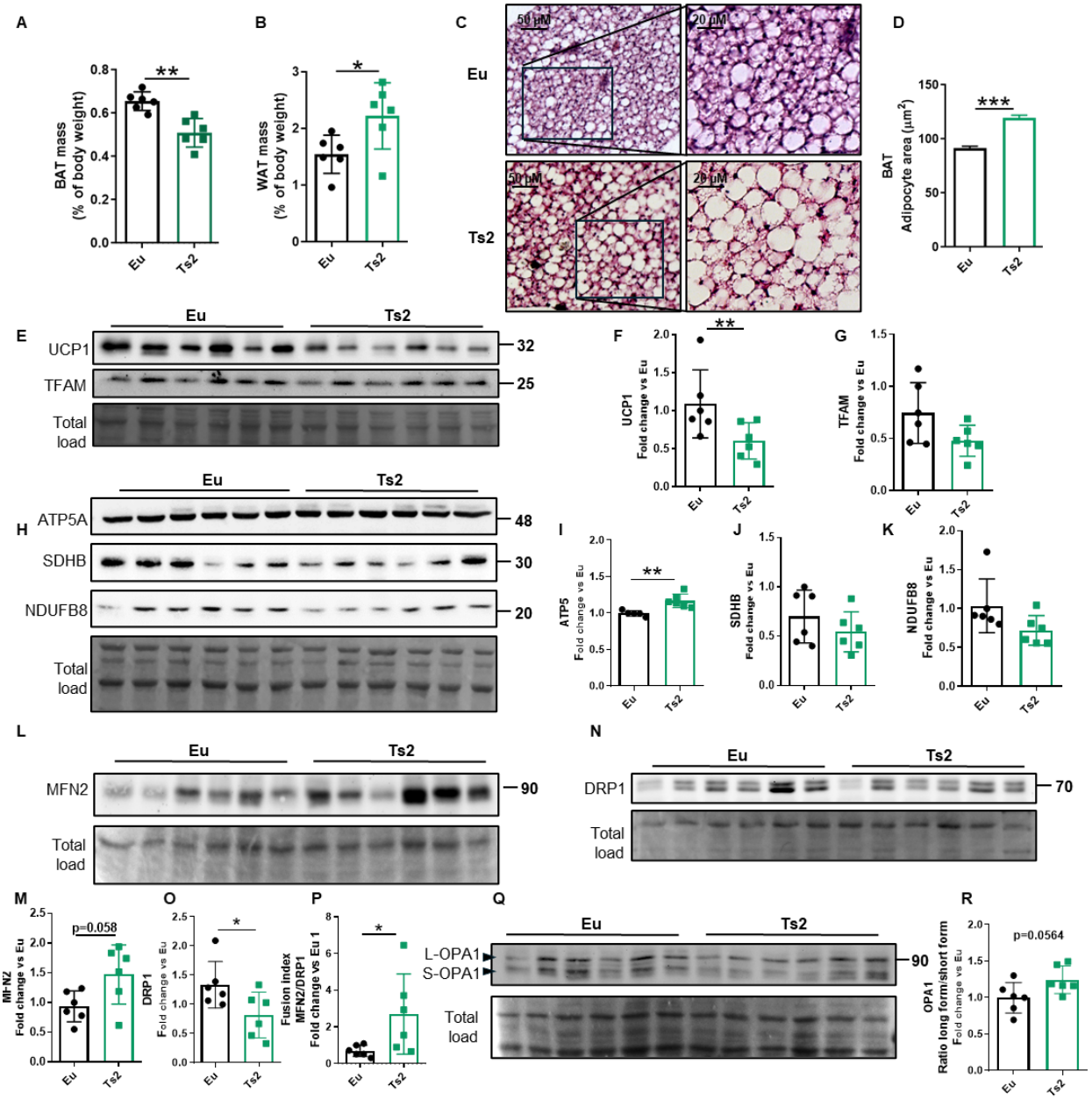

Figure 1. BAT of DS mice shows signs of the whitening process.

Mass of (**A**) BAT and (**B**) visceral WAT expressed as percentage of body weight. (**C**) Representative images of BAT from Ts2 mice after staining with H&E. Scale bars, 50 µm and 20 µm for magnifications. (**E**) The bar graph shows lipid droplets (LDs) diameter measured in at least 3 fields for each image through ImageJ. (**E-G**) Western blot and densitometric analyses of UCP1 and TFAM levels in BAT. (**H-K**) Western blot and densitometric analyses of ATP5A, SDHB, NDUFB8 levels in BAT. (**L, M**) Western blot and densitometric analyses of MNF2 levels in BAT. (**N, O**) Western blot and densitometric analyses of DRP1 levels in BAT. (**P**) Fusion index calculated as ratio between MNF2 and DRP1 levels. (**Q-R**) Western blot and densitometric analyses of OPA1 long to short ratio in BAT. Total load was used for protein normalization in all western blot analyses. Data are shown

as fold change vs Eu sample 1 (Eu1) ± sd (n=6 in each group; * $p < 0.05$ vs Eu1; ** $p < 0.01$ *vs.* Eu1; *** $p < 0.001$ *vs.* Eu1).

BAT from Ts2Cje mice displays impaired activation of metabolic pathways essential for thermogenesis

We next investigated whether the phenotypic and molecular alterations observed in BAT from Ts2 mice were associated with compromised activation of metabolic pathways that support thermogenic function. Brown adipocytes depend on the coordinated oxidation of fatty acids and glucose to sustain mitochondrial respiration and heat production. Assessment of the lipolytic pathway revealed a marked reduction in the expression of adipose triglyceride lipase (ATGL) –the rate-limiting enzyme in triacylglycerol hydrolysis– as well as of hormone-sensitive lipase (HSL), in BAT from Ts2 mice compared to Eu controls (Figure 2A–C). Consistent with impaired lipid mobilization, we also found that the N-acetylaspartate (NAA) metabolic pathway –previously shown to enhance triacylglycerol turnover and thermogenesis in brown adipocytes [12]– was downregulated in Ts2 mice. Specifically, expression of the NAA-synthesizing enzyme N-acetyltransferase 8-like (NAT8L) was significantly decreased (Figure 2D, E), while the levels of the NAA-catabolizing enzyme aspartoacylase (ASPA) remained unchanged (Figure 2D, F).

Glucose metabolism was likewise affected. Increased phosphorylation of the pyruvate dehydrogenase E1-alpha (PDH-E1α) subunit at the inhibitory site indicated a reduced mitochondrial flux of pyruvate, suggesting impaired glucose oxidation in BAT from Ts2 mice (Figure 2G, H). In parallel, insulin signaling was markedly attenuated, as evidenced by reduced phosphorylation of the insulin receptor (IR) (Figure 2I, J) and decreased activation of AKT at both Ser473 and Thr308 sites (Figure 2K–M).

Together, these findings demonstrate that BAT from Ts2 mice is metabolically reprogrammed toward a less oxidative phenotype, with impaired lipid and glucose utilization, blunted insulin signaling, and downregulation of pathways that are critical for thermogenic activation. These metabolic deficits are likely to contribute to the reduced thermogenic competence and increased susceptibility to metabolic dysfunction in DS.

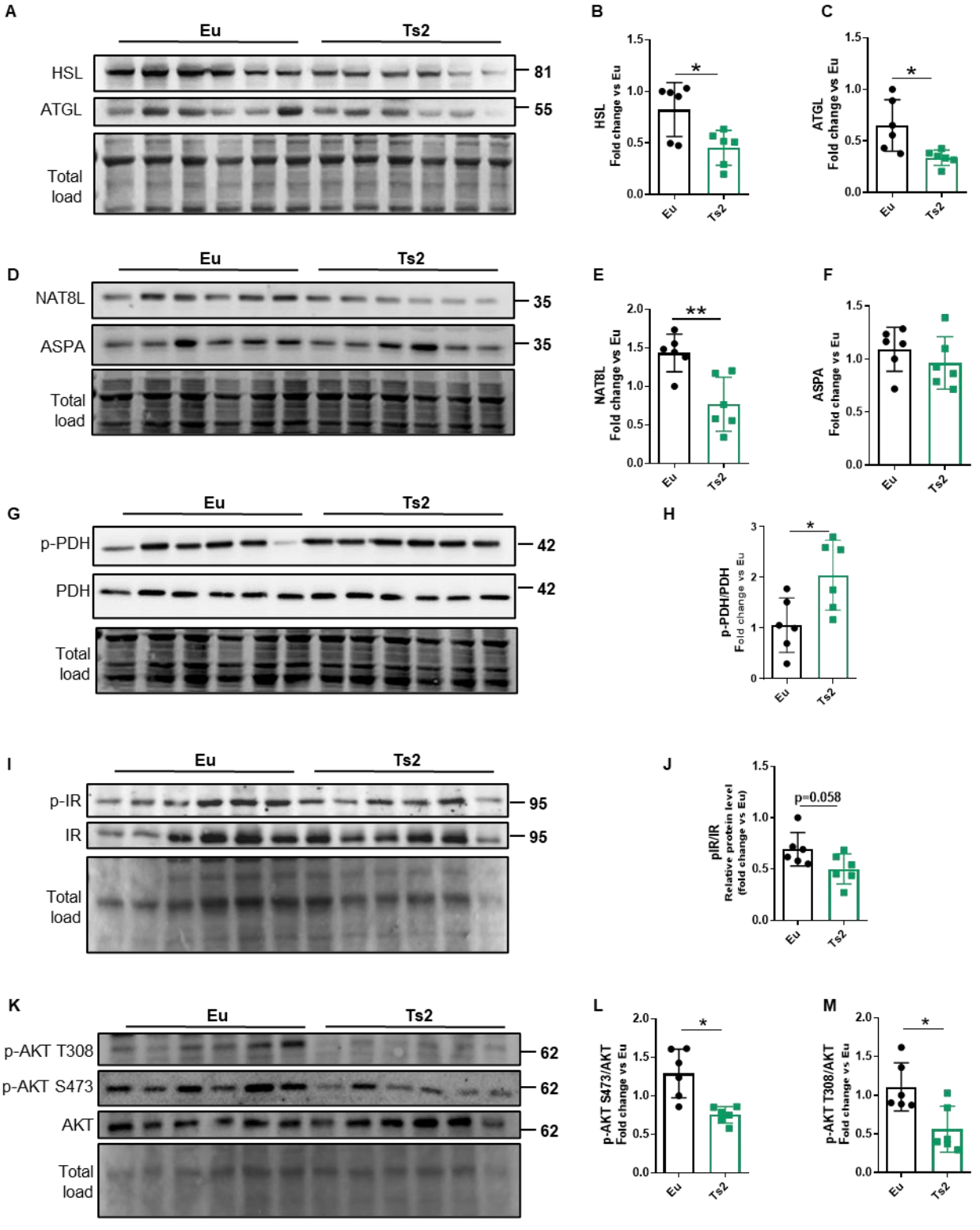

Figure 2. BAT of DS mice shows a decrease in the metabolic pathways that boost thermogenesis. (**A-C**) Western blot and densitometric analyses of HSL and ATGL levels in BAT. (**D-F**) Western blot and densitometric analyses of ASPA and NAT8L levels in BAT. (**G, H**) Western blot and densitometric analyses of p- PDHE1α (S300) and PDHE1α levels in BAT. (**I, J**) Western blot and densitometric analyses of p-IR in BAT. (**K-M**) Western blot and densitometric analyses of p-AKT

(S473 and T308) and AKT in BAT. Total load was used for protein normalization in all western blot analyses. Data are shown as fold change vs Eu sample 1 (Eu1) ± sd (n=6 in each group; * $p < 0.05$ vs Eu1; ** $p < 0.01$ *vs.* Eu1).

BAT from Ts2Cje mice exhibits oxidative stress

Multiple mechanisms have been implicated in the whitening of BAT under obese and pathological conditions, including endoplasmic reticulum (ER) stress, hypoxia, and inflammation [8,13]. In BAT from Ts2 mice, we did not observe significant alterations in ER stress marker CHOP, hypoxia-inducible factor HIF1α, or the phosphorylation status of the inflammatory transcription factor NF-κB p65 (Figure 3A–F). In contrast, markers of oxidative stress were markedly elevated in Ts2 mice. Immunodetection of 4-hydroxynonenal (4-HNE)-protein adducts –stable products of lipid peroxidation– revealed a significant increase in BAT from Ts2 mice (Figure 3G, H). This increase was accompanied by an altered antioxidant enzyme profile: while catalase (CAT) expression was reduced, SOD1 and mitochondrial superoxide dismutase 2 (SOD2) were significantly upregulated (Figure 3I–L). This pattern suggests an unbalanced antioxidant response, with increased dismutation of superoxide potentially leading to accumulation of downstream peroxides.

Because 4-HNE accumulation is a key mediator of ferroptosis, we next assessed major components of the lipid peroxide detoxification machinery. Glutathione peroxidase 4 (GPX4), a central inhibitor of ferroptosis via reduction of lipid hydroperoxides, was significantly downregulated in Ts2 BAT (Figure 3M, N). Conversely, the expression of ferroptosis suppressor protein-1 (FSP1), which provides a CoQ10-dependent antioxidant defense, was markedly upregulated (Figure 3M, O). Expression of BACH1, a transcriptional repressor that promotes ferroptosis by limiting antioxidant gene expression, was not significantly altered (Figure 3P, Q).

To better understand the interplay between redox imbalance and the other markers that can drive BAT whitening, we performed correlation analyses. Strong positive correlations were observed between 4-HNE, HIF1α, SOD1, and FSP1. Although weaker, a positive correlation was also noted between 4-HNE, FSP1, SOD2 and BACH1. Conversely, SOD2 and CAT exhibited a negative correlation, supporting the hypothesis of an antioxidant system in disequilibrium (Figure 3R).

Collectively, these findings highlight a pronounced redox imbalance in BAT of Ts2 mice, characterized by increased lipid peroxidation, altered antioxidant enzyme expression, and dysregulation of ferroptosis-related pathways. These redox alterations likely contribute to the whitening phenotype and may represent a mechanistic link between trisomy-driven oxidative stress and impaired thermogenic function.

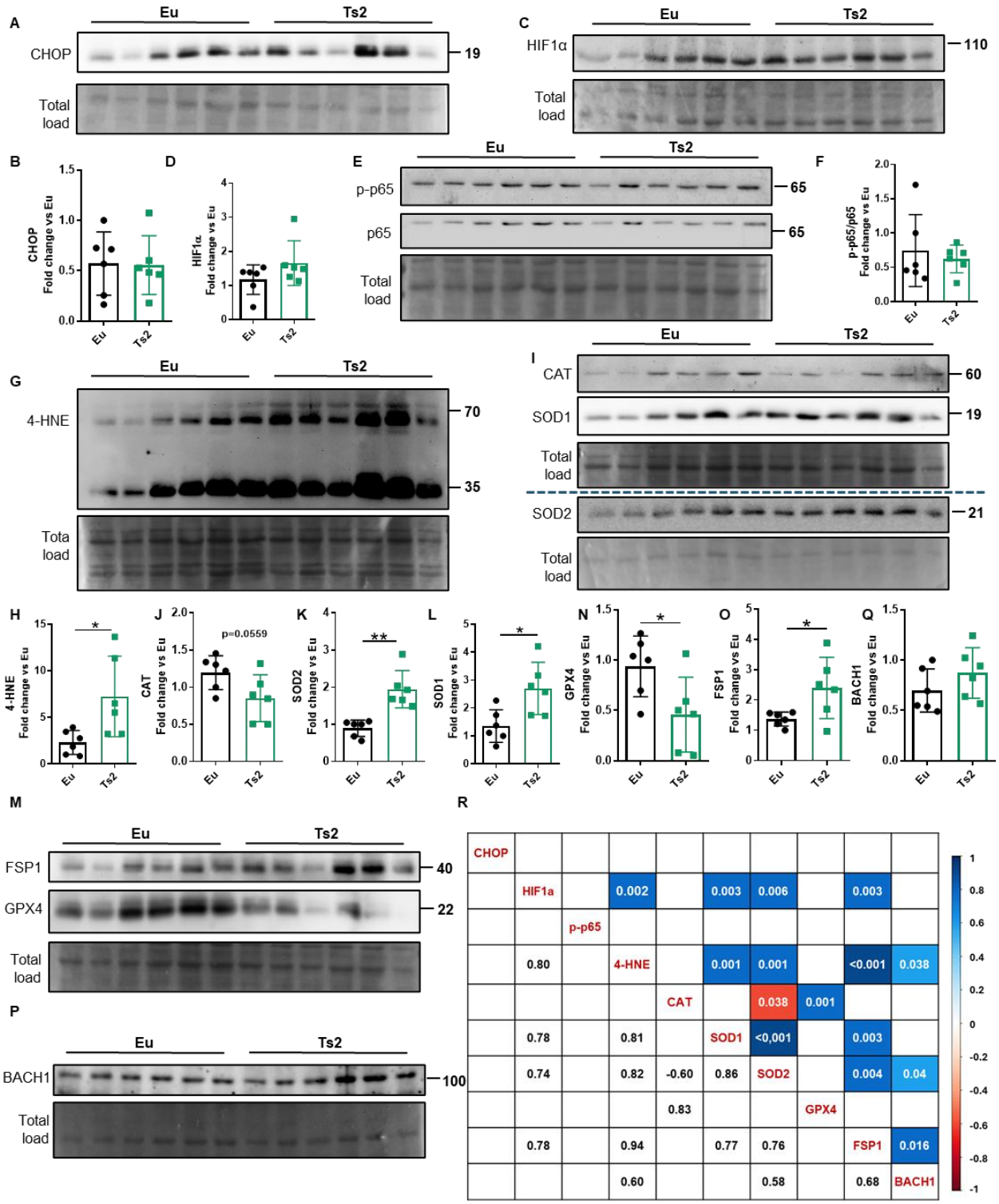

Figure 3. BAT of DS mice shows signs of oxidative stress and antioxidant imbalance.

(**A, B**) Western blot and densitometric analyses of CHOP levels in BAT. (**C, D**) Western blot and densitometric analyses of HIF1α levels in BAT. (**E, F**) Western blot and densitometric analyses of p-p65 (S536) and p65 levels in BAT. (**G, H**) Western blot and densitometric analyses of 4-HNE levels in BAT. (**I-L**) Western blot and densitometric analyses of CAT, SOD1 and SOD2 levels in BAT. (**M-O**) Western blot and densitometric analyses of FSP1 and GPX4 levels in BAT. (**P, Q**) Western blot

and densitometric analyses of BACH1 levels in BAT. Total load was used for protein normalization in all western blot analyses. (**R**) Correlation analysis of BAT protein expression in Eu1 and DS mice. Data are shown as fold change vs Eu sample 1 (Eu1) ± sd (n=6 in each group; * $p < 0.05$ vs Eu1).

Subcutaneous white adipose tissue from Ts2Cje mice exhibits oxidative stress, senescence, and inflammation

In addition to BAT, we focused the attention on sWAT, a depot enriched in thermogenic beige adipocytes under physiological stimuli. Dysfunctional sWAT is often characterized by cellular senescence and chronic low-grade inflammation [15]. The pronounced β-galactosidase staining in sWAT from Ts2 mice is indicative of enhanced cellular senescence (Figure 4A). This was corroborated by increased expression of the cyclin-dependent kinase inhibitor p21 (Figure 4B, C). In parallel, we observed elevated levels of the proinflammatory transcription factor NF-κB p65 and its downstream targets, tumor necrosis factor alpha (TNFα) and inducible nitric oxide synthase (iNOS), in Ts2 sWAT (Figure 4B, D–F), pointing to a senescence-associated secretory phenotype (SASP). The upregulation of Interleukin 6 (IL6) was not statistically significant (Figure 4B, E).

Consistent with findings in BAT, oxidative stress markers were significantly elevated in Ts2 sWAT. Levels of 4-HNE were markedly increased (Figure 4H, I), along with elevated expression of both SOD1 and SOD2 (Figure 4J, L, M). While CAT levels remained unchanged in this depot (Figure 4J, K), GPX4 and FSP1 were significantly upregulated in Ts2 mice (Figure 4N–P), possibly reflecting a compensatory response to increased oxidative lipid damage. Correlation analyses revealed that GPX4 and FSP1 expression positively correlated with NF-κB p65 and TNFα. Furthermore, SOD1 expression strongly correlated with 4-HNE, p21, and p65 (Figure 4Q), highlighting a coordinated network of oxidative stress, cellular senescence, and inflammatory signaling in Ts2 sWAT.

These results indicate that sWAT in Ts2 mice undergoes profound redox and inflammatory remodeling, marked by increased lipid peroxidation, activation of senescence pathways, and ferroptosis-related adaptations. This altered environment may also impact the thermogenic potential of beige adipocytes and contribute to systemic metabolic dysfunction in DS.

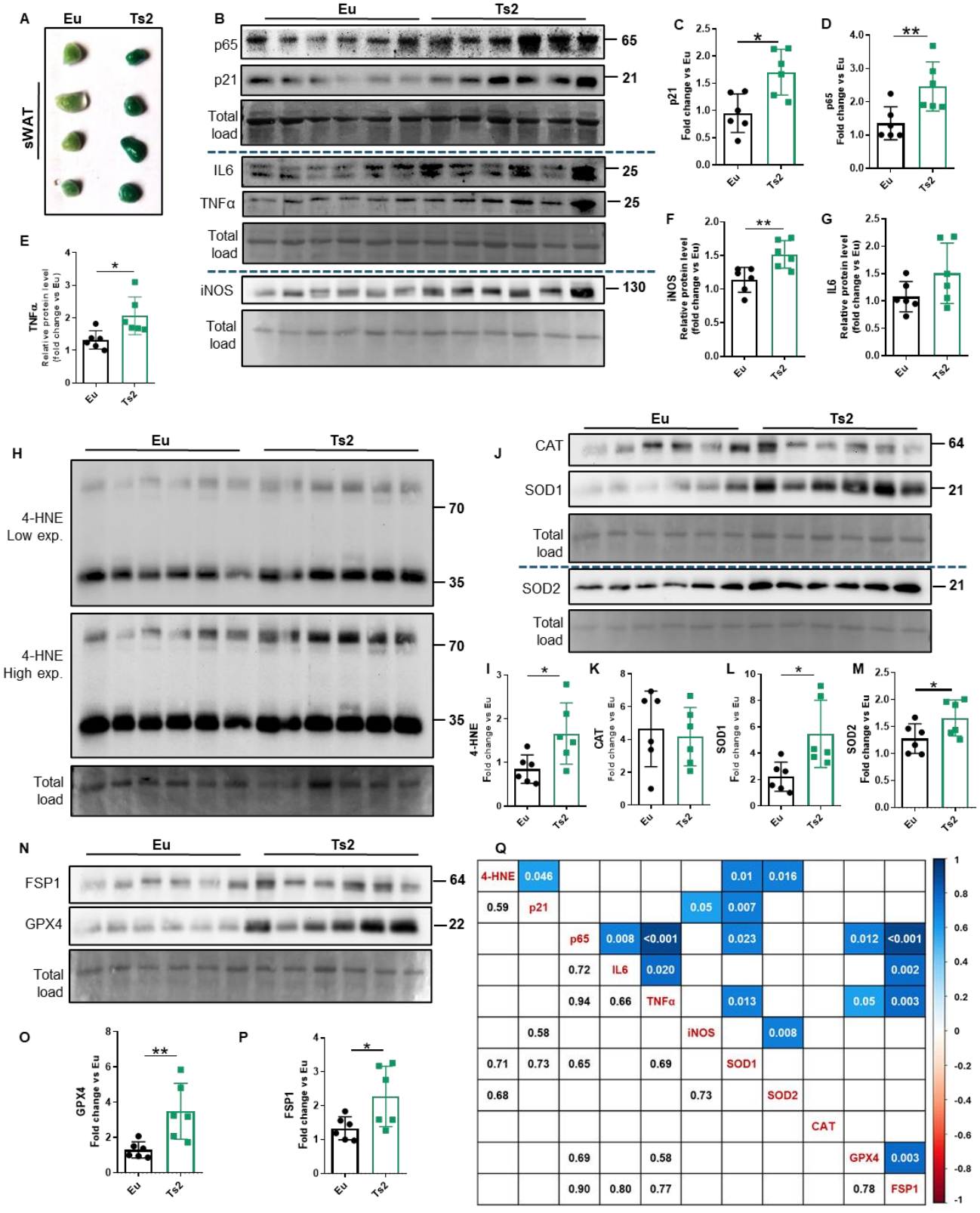

Figure 4. DS mice also show oxidative stress and sWAT dysfunction

(**A**) Representative images of Eu and Ts2 biopsies of sWAT used for senescence β-Galactosidase staining. (**B-G**) Western blot and densitometric analyses of p65, p21, IL6, TNFα and iNOS levels in BAT. (**H, I**) Western blot and densitometric analyses of 4-HNE levels in BAT. (**J-M**) Western blot and densitometric analyses of CAT, SOD1 and SOD2 levels in BAT. (**N-P**) Western blot and densitometric analyses of FSP1 and GPX4 levels in BAT. Total load was used for protein normalization in all western blot analyses. (**Q**) Correlation analysis of sWAT protein expression in Eu1 and DS mice. Data are shown as fold change vs Eu sample 1 (Eu1) ± sd (n=6 in each group; * $p < 0.05$ vs Eu1; ** $p < 0.01$ *vs.* Eu1).

Discussion

Our findings reveal a profound dysfunction of thermogenic adipose tissues in the Ts2 mouse model of DS, characterized by morphological and molecular hallmarks of BAT whitening. DS BAT displayed the classical phenotypic switch from multilocular to unilocular lipid droplets, along with adipocyte hypertrophy and a significant reduction in UCP1 expression, consistent with the loss of thermogenic identity typically seen under obesogenic conditions [7,8]. It is known that ATP synthase levels in BAT are generally lower compared to other ETC components [16], but DS BAT shows the upregulation of ATP synthase and no significant alteration ETC complexes. Given that uncoupling via UCP1 is central to BAT thermogenesis, the concurrent reduction in UCP1 and increase in ATP synthase levels suggest a shift toward more efficient ATP production at the expense of thermogenic proton leak, indicating impaired mitochondrial uncoupling. The reduction in the mitochondrial fission marker DRP1 is another feature that confirms BAT whitening in DS mice. In fact, the fission process is fundamental for preserving functional mitochondria with intense uncoupling activity [17]. Considering that the mitochondrial fragmentation due to cold exposure is associated with the accumulation of the proteolytic isoform S-OPA1, the shift in the balance of OPA-1 isoforms toward the full-length one (L-OPA1) further supports a reduced fission process in DS mice [11].

From a metabolic standpoint, BAT thermogenesis relies on the oxidation of both glucose and fatty acids. The downregulation of key lipolytic enzymes suggests a reduced mobilization and utilization of lipid stores, potentially explaining the observed lipid droplet enlargement. This phenotype mirrors that of ATGL-deficient mice, which also exhibit BAT whitening [7]. Interestingly, the deactivation of the lipolytic pathway is associated with the reduced expression of the NAA-producing enzyme NAT8L, which was shown to be altered also in the adipose tissue of amyotrophic lateral sclerosis

model [18]. Given NAA's role in promoting lipid utilization and thermogenesis in BAT [12], this finding further corroborates that BAT in DS loses its typical thermogenic features. Glucose oxidation is similarly compromised in Ts2 BAT, as indicated by enhanced inhibitory phosphorylation of the PDH complex. This inhibition may stem from impaired AKT signaling [19], a pathway crucial for insulin-stimulated glucose uptake and thermogenesis in brown adipocytes [20]. Consistently, insulin signaling is attenuated in DS BAT as demonstrated by the reduced phosphorylation of AKT and IR. As BAT counteracts T2D pathogenesis favouring glucose disposal and insulin sensitivity also in humans [21], future studies may clarify whether BAT dysmetabolism can contribute to insulin resistance phenotype in DS individuals.

Oxidative stress emerged as a major driver of BAT dysfunction in DS. Increased levels of 4-HNE point to heightened lipid peroxidation, positively correlated with elevated HIF-1α and SOD1 expression. High levels of SOD and lipid peroxidation were also shown in DS human B lymphocytes [22] and in the erythrocytes of T2D patients [23]. Overexpression of SOD1 in DS promotes excessive H_2O_2 production, especially when not efficiently detoxified by CAT, whose levels were found to be decreased in Ts2 BAT. The accumulation of H_2O_2 facilitates iron-catalyzed Fenton reactions, further amplifying lipid peroxidation [24], a mechanism also implicated in DS-associated neurodegeneration [25]. In response to redox imbalance, Ts2 BAT upregulated FSP1, a key inhibitor of ferroptosis, possibly compensating for the observed reduction in GPX4 and supporting adipocyte survival during oxidative stress. This antioxidant shift may account for mitochondrial coupling and reduction of insulin signaling permitting thus brown-to-white conversion of adipocytes, rather than ferroptotic cell death (Figure 5). Similar molecular signatures of oxidative distress and antioxidant adaptation were also evident in sWAT, the depot containing beige adipocytes. In Ts2 mice, sWAT exhibited inflammatory and senescent traits, positively correlated with SOD1 expression. These findings are consistent with the pro-inflammatory adipose tissue phenotype described in other DS models, such as Ts65Dn [5], and contribute to the chronic low-grade inflammation that is typically linked to the development of obesity.

The phenotypic decline observed in both BAT and sWAT in Ts2 mice parallels alterations associated with aging and age-related metabolic disorders [6,26]. BAT dysfunction, increased oxidative stress, and systemic inflammation are shared features of both DS and elderly populations, underscoring the concept of DS as a segmental progeroid syndrome [27]. Given the key role of BAT in promoting insulin sensitivity and energy expenditure, strategies aimed at restoring BAT function and redox balance –via nutritional or pharmacological interventions– hold promise for mitigating metabolic

dysfunction in DS. Enhancing BAT thermogenesis may represent a novel therapeutic approach to improve metabolic health, extend lifespan, and promote healthy aging in individuals with DS.

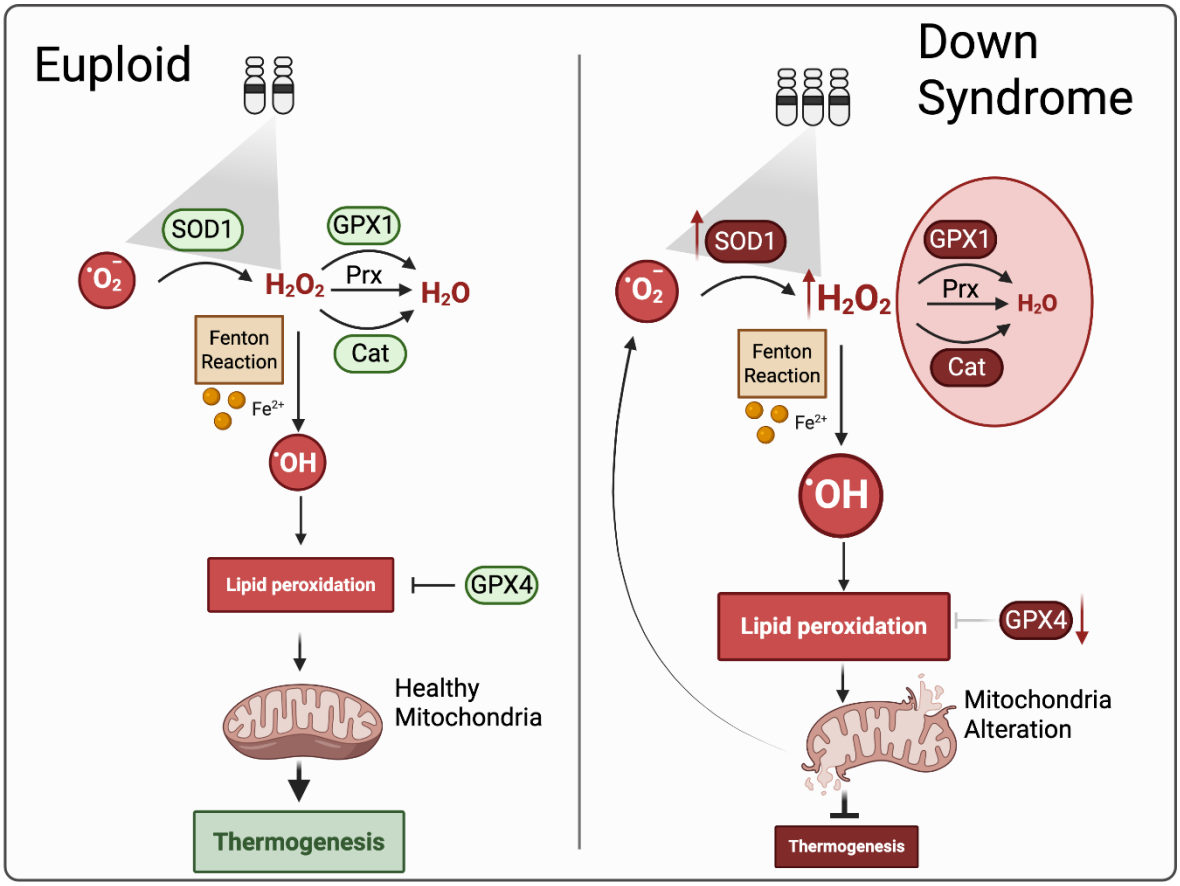

Figure 5. Schematic view of the proposed mechanism.

Overexpression of SOD1 in DS promotes excessive H_2O_2 production due to impaired detoxification by CAT that resulted to be decreased in Ts2 BAT. The accumulation of H_2O_2 facilitates iron-catalyzed Fenton reactions leading to lipid peroxidation that is further amplified by GPX downregulation. In response to the accumulation of oxidative damage, FSP1 is upregulated in Ts2 BAT possibly inhibiting ferroptosis. The oxidative distress deriving from this antioxidant shift in DS BAT may account for mitochondrial coupling and reduction of insulin signaling.

CRediT authorship contribution statement

Fabio Ciccarone: Conceptualization, Supervision, Data curation, Writing- Original draft preparation designed the experiments, Funding acquisition; Serena Castelli: Methodology, Data curation, Formal analysis, Software; Maria Rosa Ciriolo: Writing- Reviewing and Editing, Funding acquisition; Maria Giulia Bacalini: Software, Writing- Reviewing and Editing; Antonella Tramutola and Marzia Perluigi: Writing- Reviewing and Editing. All authors read and approved the final manuscript.

Conflict of interests

Authors declare no conflict of interests.

Acknowledgements

This work was partially supported by: Italian Ministry of Health - Ricerca Corrente; Italian Ministry of Health - Ricerca Finalizzata Giovani Ricercatori GR-2019-12369983; #NEXTGENERATIONEU (NGEU) funded by the Ministry of University and Research (MUR), National Recovery and Resilience Plan (NRRP), project MNESYS (PE0000006) – (DN. 1553 11.10.2022)

References

[1] S.E. Antonarakis, Down syndrome and the complexity of genome dosage imbalance, Nat Rev Genet 18 (2017) 147–163. https://doi.org/10.1038/nrg.2016.154.
[2] E. Barone, A. Arena, E. Head, D.A. Butterfield, M. Perluigi, Disturbance of redox homeostasis in Down Syndrome: Role of iron dysmetabolism, Free Radic Biol Med 114 (2018) 84–93. https://doi.org/10.1016/j.freeradbiomed.2017.07.009.
[3] M. Dierssen, M. Fructuoso, M. Martínez de Lagrán, M. Perluigi, E. Barone, Down Syndrome Is a Metabolic Disease: Altered Insulin Signaling Mediates Peripheral and Brain Dysfunctions, Front Neurosci 14 (2020) 670. https://doi.org/10.3389/fnins.2020.00670.
[4] F. Bertapelli, K. Pitetti, S. Agiovlasitis, G. Guerra-Junior, Overweight and obesity in children and adolescents with Down syndrome-prevalence, determinants, consequences, and interventions: A literature review, Res Dev Disabil 57 (2016) 181–192. https://doi.org/10.1016/j.ridd.2016.06.018.
[5] D.C. Sarver, C. Xu, L.M. Velez, S. Aja, A.E. Jaffe, M.M. Seldin, R.H. Reeves, G.W. Wong, Dysregulated systemic metabolism in a Down syndrome mouse model, Mol Metab 68 (2023) 101666. https://doi.org/10.1016/j.molmet.2022.101666.
[6] E. Zoico, S. Rubele, A. De Caro, N. Nori, G. Mazzali, F. Fantin, A. Rossi, M. Zamboni, Brown and Beige Adipose Tissue and Aging, Front Endocrinol (Lausanne) 10 (2019) 368. https://doi.org/10.3389/fendo.2019.00368.
[7] P. Kotzbeck, A. Giordano, E. Mondini, I. Murano, I. Severi, W. Venema, M.P. Cecchini, E.E. Kershaw, G. Barbatelli, G. Haemmerle, R. Zechner, S. Cinti, Brown adipose tissue whitening leads to brown adipocyte death and adipose tissue inflammation, J Lipid Res 59 (2018) 784–794. https://doi.org/10.1194/jlr.M079665.

[8] M. Alcalá, M. Calderon-Dominguez, E. Bustos, P. Ramos, N. Casals, D. Serra, M. Viana, L. Herrero, Increased inflammation, oxidative stress and mitochondrial respiration in brown adipose tissue from obese mice, Sci Rep 7 (2017) 16082. https://doi.org/10.1038/s41598-017-16463-6.
[9] J. Phan, M.A. Hickey, P. Zhang, M.-F. Chesselet, K. Reue, Adipose tissue dysfunction tracks disease progression in two Huntington's disease mouse models, Hum Mol Genet 18 (2009) 1006–1016. https://doi.org/10.1093/hmg/ddn428.
[10] F. Ciccarone, S. Castelli, G. Lazzarino, S. Scaricamazza, R. Mangione, S. Bernardini, S. Apolloni, N. D'Ambrosi, A. Ferri, M.R. Ciriolo, Lipid catabolism and mitochondrial uncoupling are stimulated in brown adipose tissue of amyotrophic lateral sclerosis mouse models, Genes Dis 10 (2023) 321–324. https://doi.org/10.1016/j.gendis.2022.04.006.
[11] Y. Ge, X. Shi, S. Boopathy, J. McDonald, A.W. Smith, L.H. Chao, Two forms of Opa1 cooperate to complete fusion of the mitochondrial inner-membrane, Elife 9 (2020) e50973. https://doi.org/10.7554/eLife.50973.
[12] A.R. Pessentheiner, H.J. Pelzmann, E. Walenta, M. Schweiger, L.N. Groschner, W.F. Graier, D. Kolb, K. Uno, T. Miyazaki, A. Nitta, D. Rieder, A. Prokesch, J.G. Bogner-Strauss, NAT8L (N-acetyltransferase 8-like) accelerates lipid turnover and increases energy expenditure in brown adipocytes, J Biol Chem 288 (2013) 36040–36051. https://doi.org/10.1074/jbc.M113.491324.
[13] I. Shimizu, T. Aprahamian, R. Kikuchi, A. Shimizu, K.N. Papanicolaou, S. MacLauchlan, S. Maruyama, K. Walsh, Vascular rarefaction mediates whitening of brown fat in obesity, J Clin Invest 124 (2014) 2099–2112. https://doi.org/10.1172/JCI71643.
[14] K. Bersuker, J.M. Hendricks, Z. Li, L. Magtanong, B. Ford, P.H. Tang, M.A. Roberts, B. Tong, T.J. Maimone, R. Zoncu, M.C. Bassik, D.K. Nomura, S.J. Dixon, J.A. Olzmann, The CoQ oxidoreductase FSP1 acts parallel to GPX4 to inhibit ferroptosis, Nature 575 (2019) 688–692. https://doi.org/10.1038/s41586-019-1705-2.
[15] T. Kawai, M.V. Autieri, R. Scalia, Adipose tissue inflammation and metabolic dysfunction in obesity, Am J Physiol Cell Physiol 320 (2021) C375–C391. https://doi.org/10.1152/ajpcell.00379.2020.
[16] T.V. Kramarova, I.G. Shabalina, U. Andersson, R. Westerberg, I. Carlberg, J. Houstek, J. Nedergaard, B. Cannon, Mitochondrial ATP synthase levels in brown adipose tissue are governed by the c-Fo subunit P1 isoform, FASEB J 22 (2008) 55–63. https://doi.org/10.1096/fj.07-8581com.
[17] Y. Ibayashi, N. Hasuzawa, S. Nomura, M. Kabashima, A. Nagayama, S. Iwata, M. Kitamura, K. Ashida, Y. Moriyama, K. Yamamoto, M. Nomura, L. Wang, Mitochondrial fission is required for thermogenesis in brown adipose tissue, PLoS One 19 (2024) e0312352. https://doi.org/10.1371/journal.pone.0312352.
[18] S. Castelli, E. Desideri, L. Laureti, F. Felice, A. De Cristofaro, S. Scaricamazza, G. Lazzarino, M.R. Ciriolo, F. Ciccarone, N-acetylaspartate promotes glycolytic-to-oxidative fiber-type switch and resistance to atrophic stimuli in myotubes, Cell Death Dis 15 (2024) 686. https://doi.org/10.1038/s41419-024-07047-0.
[19] G.J. Cerniglia, S. Dey, S.M. Gallagher-Colombo, N.A. Daurio, S. Tuttle, T.M. Busch, A. Lin, R. Sun, T.V. Esipova, S.A. Vinogradov, N. Denko, C. Koumenis, A. Maity, The PI3K/Akt Pathway Regulates Oxygen Metabolism via Pyruvate Dehydrogenase (PDH)-E1α Phosphorylation, Mol Cancer Ther 14 (2015) 1928–1938. https://doi.org/10.1158/1535-7163.MCT-14-0888.
[20] V. Albert, K. Svensson, M. Shimobayashi, M. Colombi, S. Muñoz, V. Jimenez, C. Handschin, F. Bosch, M.N. Hall, mTORC2 sustains thermogenesis via Akt-induced glucose uptake and glycolysis in brown adipose tissue, EMBO Mol Med 8 (2016) 232–246. https://doi.org/10.15252/emmm.201505610.

[21] M. Chondronikola, E. Volpi, E. Børsheim, C. Porter, P. Annamalai, S. Enerbäck, M.E. Lidell, M.K. Saraf, S.M. Labbe, N.M. Hurren, C. Yfanti, T. Chao, C.R. Andersen, F. Cesani, H. Hawkins, L.S. Sidossis, Brown adipose tissue improves whole-body glucose homeostasis and insulin sensitivity in humans, Diabetes 63 (2014) 4089–4099. https://doi.org/10.2337/db14-0746.

[22] K. Mouli, A.V. Liopo, L.J. Suva, K.R. Olson, E.A. McHugh, J.M. Tour, P.J. Derry, T.A. Kent, SOD1 Is an Integral Yet Insufficient Oxidizer of Hydrogen Sulfide in Trisomy 21 B Lymphocytes and Can Be Augmented by a Pleiotropic Carbon Nanozyme, Antioxidants (Basel) 13 (2024) 1361. https://doi.org/10.3390/antiox13111361.

[23] S. de M. Bandeira, G. da S. Guedes, L.J.S. da Fonseca, A.S. Pires, D.P. Gelain, J.C.F. Moreira, L.A. Rabelo, S.M.L. Vasconcelos, M.O.F. Goulart, Characterization of blood oxidative stress in type 2 diabetes mellitus patients: increase in lipid peroxidation and SOD activity, Oxid Med Cell Longev 2012 (2012) 819310. https://doi.org/10.1155/2012/819310.

[24] H. Yang, F. Tai, T. Wang, X. Zheng, C. Ge, Y. Qin, H. Fu, Hydrogen peroxide and iron ions can modulate lipid peroxidation, apoptosis, and the cell cycle, but do not have a significant effect on DNA double-strand break, Biochem Biophys Res Commun 651 (2023) 121–126. https://doi.org/10.1016/j.bbrc.2023.02.023.

[25] M.A. Thorwald, J.A. Godoy-Lugo, E. Kerstiens, G. Garcia, M. Kim, S.J. Shemtov, J. Silva, S. Durra, P.A. O'Day, W.J. Mack, A. Hiniker, M. Vermulst, B.A. Benayoun, R. Higuchi-Sanabria, H.J. Forman, E. Head, C.E. Finch, Down syndrome with Alzheimer's disease brains have increased iron and associated lipid peroxidation consistent with ferroptosis, bioRxiv (2025) 2025.02.05.636731. https://doi.org/10.1101/2025.02.05.636731.

[26] L.F. Gonçalves, T.Q. Machado, C. Castro-Pinheiro, N.G. de Souza, K.J. Oliveira, C. Fernandes-Santos, Ageing is associated with brown adipose tissue remodelling and loss of white fat browning in female C57BL/6 mice, Int J Exp Pathol 98 (2017) 100–108. https://doi.org/10.1111/iep.12228.

[27] W.B. Zigman, Atypical aging in Down syndrome, Dev Disabil Res Rev 18 (2013) 51–67. https://doi.org/10.1002/ddrr.1128.